Inorganic Interfaces

DOI: 10.1002/anie.201402026

All-Inorganic Nanocrystals as a Glue for BiSbTe Grains: Design of Interfaces in Mesostructured Thermoelectric Materials**

*Jae Sung Son, Hao Zhang, Jaeyoung Jang, Bed Poudel, Al Waring, Luke Nally, and Dmitri V. Talapin**

Abstract: *Nano- and mesostructuring is widely used in thermoelectric (TE) materials. It introduces numerous interfaces and grain boundaries that scatter phonons and decrease thermal conductivity. A new approach has been developed for the rational design of the interfaces in TE materials by using all-inorganic nanocrystals (NCs) that serve as a "glue" for mesoscopic grains. For example, circa 10 nm Bi NCs capped with $(N_2H_5)_4Sb_2Te_7$ chalcogenidometallate ligands can be used as an additive to BiSbTe particles. During heat treatment, NCs fill up the voids between particles and act as a "glue", joining grains in hot-pressed pellets or solution-processed films. The chemical design of NC glue allowed the selective enhancement or decrease of the majority-carrier concentration near the grain boundaries, and thus resulted in doped or de-doped interfaces in granular TE material. Chemically engineered interfaces can be used as to optimize power factor and thermal conductivity.*

In the last decade, nano- and mesostructuring of thermoelectric (TE) materials has become a new paradigm to enhance the efficiency of TE devices.[1] Various approaches such as spinodal decomposition during solid-state synthesis[2] and consolidation of nanopowders[3] have been used to prepare nanostructured materials with high TE efficiency, which is characterized by the dimensionless figure-of-merit $ZT = (S^2\sigma/k)T$, where σ, S, k, and T are the electrical conductivity, Seebeck coefficient, thermal conductivity, and absolute temperature, respectively.[4] Switching from TE materials with large crystal grains to nano- and mesostructured compounds brings up fundamentally important problems related to morphological stability, grain growth, and inter-grain transport. For example, the consolidation of grains into a dense phase by spark plasma sintering or hot-pressing is often accompanied by substantial grain growth, decreasing the positive effect of grain boundaries. Moreover, in a granular material ZT is strongly dependent on electronic and thermal transport through the grain boundaries.[4,5] At the same time, the chemistry and physics of interfaces in TE devices remains largely underexplored.[6] This is in stark contrast to thin-film photovoltaics where grain boundaries have been studied in depth for many years.[7] Improved passivation of CdTe grains with $CdCl_2$ and Cu^+,[8] or CIGS grains with Na^+[9] has doubled the efficiency of corresponding solar cells. Compared to semiconductors used in solar cells, heavily doped TE materials should be less sensitive to trapping carriers at the interfaces. However, because the current path in TE devices is large (mm scale) compared to thin film solar cells (ca. 10^{-6} m), even minor interfacial resistances lead to significant losses of σ.

To address these issues, we propose the concept of "NC glue" for mesoscale particles of TE materials. The benefits of this approach are: 1) a depressed melting point of NCs, which permits the consolidation of grains at lower temperatures; and 2) by tuning the chemistry of the NC glue, we can selectively modify the grain boundaries, thus offering an additional degree of control over charge and heat transport in TE materials. Our approach uses NCs as a small (1–3 wt%) additive to traditional TE materials, which should not significantly affect the cost structure of TE modules.

$Bi_xSb_{2-x}Te_3$ provides a convenient model system to explore the effect of NC glue on TE properties. These materials exhibit high ZT values near room temperature, and the dependence of their properties on compositions and structures is relatively well-understood.[1a,3a,4,10] We employed all-inorganic Bi NCs capped with $(N_2H_5)_4Sb_2Te_7$ molecular metal chalcogenide (MCC) ligands as a glue for the consolidation of BiSbTe ball-milled particles (Figure 1a). Depending on the composition of ball-milled particles, $Sb_2Te_7^{4-}$ MCC-capped Bi NCs could either increase or decrease the concentration of majority (hole) carriers near grain boundaries in BiSbTe. This enabled tuning σ, S, and k towards optimal ZT values.

Bi NCs were synthesized by the reduction of bismuth *n*-dodecanethiolate using tri-*n*-octylphosphine as a mild reducing agent.[11] The transmission electron microscopy (TEM) image of Bi NCs showed uniform circa 10 nm-sized NCs (Figure 1b). To prepare all-inorganic NC glue for BiSbTe particles, the dodecanethiol capping ligands on as-synthesized Bi NCs were exchanged for inorganic $Sb_2Te_7^{4-}$ ligands, forming negatively charged NCs charge balanced with $N_2H_5^+$ ions.[12] Figure 1c shows that the ligand exchange did

[*] Dr. J. S. Son, H. Zhang, Dr. J. Jang, Prof. Dr. D. V. Talapin
Department of Chemistry and James Franck Institute
University of Chicago, Chicago, IL 60637 (USA)
E-mail: dvtalapin@uchicago.edu
Dr. B. Poudel, A. Waring, L. Nally
Evident Technologies Inc., Troy (USA)
Prof. Dr. D. V. Talapin
Center for Nanoscale Materials, Argonne National Lab
Argonne, IL 60439 (USA)

[**] We thank S. G. Kwon for the EDS and DSC measurements. This work was supported by the II-VI Foundation, Evident Technologies, and NSF MRSEC Program under Award Number DMR-0213745. J.S.S. and D.V.T. also thank the University of Chicago Innovation Fund. The work at the Center for Nanoscale Materials (ANL) was supported by the US Department of Energy under Contract No. DE-AC02-06CH11357.

Supporting information for this article is available on the WWW under http://dx.doi.org/10.1002/anie.201402026.

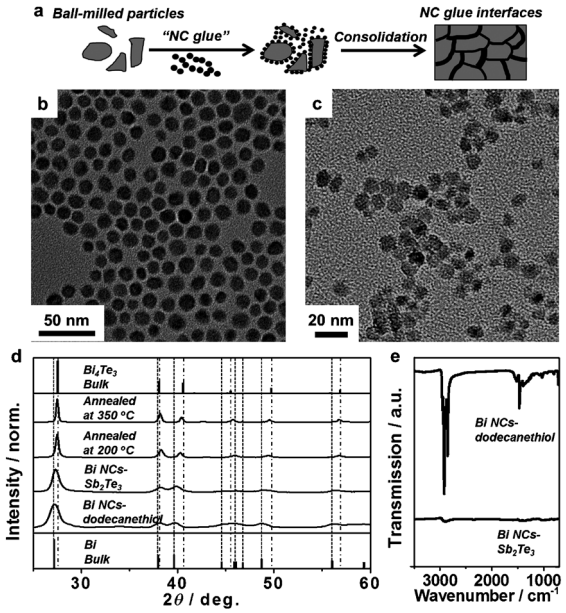

Figure 1. a) Illustration of the preparation of hierarchically structured TE materials from ball-milled particles with NC glue. TEM images of b) dodecanethiol-capped and c) $Sb_2Te_7^{4-}$-capped Bi NCs. d) XRD patterns of dodecanethiol-capped Bi NCs, and $Sb_2Te_7^{4-}$-capped Bi NCs dried at room temperature and annealed at 200 °C and 350 °C. e) FTIR spectra of dodecanethiol-capped and $Sb_2Te_7^{4-}$-capped Bi NCs.

not affect the average size and monodispersity of Bi NCs. The X-ray diffraction (XRD) analyses of dodecanethiol-capped and $Sb_2Te_7^{4-}$ MCC-capped Bi NCs (Figure 1 d) showed identical patterns corresponding to that of bulk Bi, confirming no structural or size changes caused by the ligand exchange. The FTIR spectrum of the MCC-capped NCs (Figure 1 e) showed the disappearance of the C–H stretching and bending modes that indicated almost complete replacement of the organic ligands by the inorganic ligands.

After annealing, $N_2H_5^+/Sb_2Te_7^{4-}$-capped Bi NCs formed a Bi-rich BiSbTe phase with nominal $Bi_{3.2}Sb_{0.8}Te_{2.9}$ composition, as obtained from the elemental analysis. The XRD patterns of the NCs annealed at 200 °C and 350 °C (Figure 1 d) showed sharpening and a shift of the XRD peaks to higher 2θ angles. The XRD patterns of annealed NCs closely resembled a Bi_4Te_3 phase, a layered compound containing Bi_2 and Bi_2Te_3 hexagonal layers with a 1:1 ratio.[13] Observed small shifts of some peaks to higher 2θ angles are expected owing to integration of Sb^{3+} into the structure. The differential scanning calorimetry (DSC) scan (Supporting Information, Figure S1a) showed an endothermic peak below 200 °C, which we interpreted as the melting of Bi NCs followed by their reaction with $Sb_2Te_7^{4-}$ surface ligands. The decrease in the melting point compared to bulk Bi (m.p. 271.4 °C) is in agreement with the previous report of the size effect on NC melting.[14] These results indicate that the chemical reaction between Bi NCs and inorganic MCC ligands occurred below about 200 °C and generated a Bi-rich BiSbTe phase. The thermogravimetric analysis (TGA) of $Sb_2Te_7^{4-}$ MCC-capped Bi NCs showed a negligible weight loss and volume contraction at temperatures up to 450 °C (Supporting Information, Figure S1b).

The direct sintering of BiSbTe particles requires rather high temperature (> 400 °C) that causes significant grain growth. At the same time, the low reaction temperature for the formation of a BiSbTe phase from $Sb_2Te_7^{4-}$-capped Bi NCs should allow gluing larger BiSbTe particles together at lower temperatures. To test this hypothesis, we combined MCC-capped Bi NCs with $Bi_{0.5}Sb_{1.5}Te_3$ ball-milled particles. The NCs were well attached to the surface of particles (Supporting Information, Figure S2), which suggested that the NC glue does not segregate and forms the interfaces between BiSbTe particles during consolidation. A suspension of ball-milled particles with NC glue in hydrazine was drop-cast on a glass substrate and annealed at 400 °C for 15 min, which produced a continuous BiSbTe thin film (Figure 2 a).

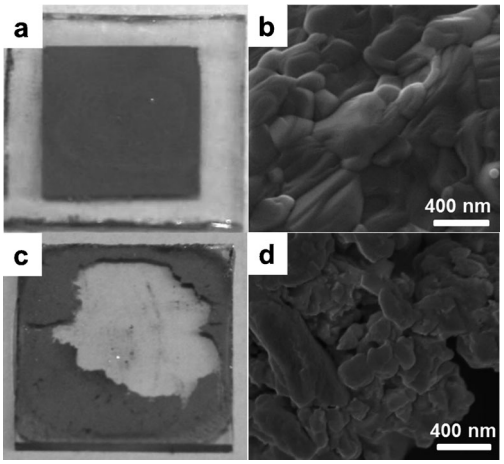

Figure 2. Photographs and SEM images of annealed $Bi_{0.5}Sb_{1.5}Te_3$ ball-milled particle thin films with a), b) and without c), d) $Sb_2Te_7^{4-}$-capped Bi NCs at 400 °C.

The SEM image in Figure 2 b shows that particles were well-fused together, with no voids between grains. It suggests that melted NCs filled in the voids and formed interfaces between mesoscale particles. Obtained thin films exhibited a relatively high electrical conductivity of 40028 $S\,m^{-1}$ and the Seebeck coefficient of 221 $\mu V\,K^{-1}$, resulting in high TE power factor $S^2\sigma = 19.6\ \mu W\,cm^{-1}\,K^{-2}$. In contrast, the particles suspension without the NCs did not form a continuous film under the same conditions. After annealing at 400 °C, the film composed of only particles remained powdery and spontaneously peeled off from the glass substrate (Figure 2 c). The SEM image showed that individual particles were only slightly sintered, and multiple voids between grains were observed (Figure 2 d). These observations clearly demonstrated the glue effect of $Sb_2Te_7^{4-}$ MCC-capped Bi NCs for ball-milled particles.

To further understand how MCC-capped NCs affect the electronic structure of interfaces and contribute to the TE characteristics of BiSbTe, we investigated the properties of pellets prepared with varying amounts of NC glue. For the first set of samples, we used powder prepared by ball-milling beads with stoichiometric $Bi_{0.5}Sb_{1.5}Te_3$ composition (further referred to as "BST") to observe the effect of NC glue on pure $Bi_{0.5}Sb_{1.5}Te_3$ grains. For the second set of experiments, elemental Bi, Sb, and Te with nominal composition

$Bi_{0.5}Sb_{1.5}Te_{3.2}$ (7% excess Te) were mixed together and mechanically reacted in a ball mill (further referred to as "BST:T" samples). These methods are common for producing *p*-type BiSbTe with small-sized grains and the optimized carrier concentration for TE applications.[10,15] The XRD patterns of both particles (Supporting Information, Figure S3) showed widened peaks in comparison to those of bulk materials, indicating a decreased size of crystalline domains. The estimated average crystalline domain sizes by the Williamson–Hall plot were 51.4 nm for BST particles and 73.4 nm for BST:T particles. To prepare the pellets, the mixed particles with the NC glue were dried and hot-pressed for 15 min at 350 °C for BST particles and 400 °C for BST:T particles (Supporting Information, Figure S4). The NC content was controllably varied from 0% to 5% in weight. The hot-pressed pellets are denoted by BST# and BST:T# (# is NC content in percentage), respectively. The relative density of all BST and BST:T samples were 92–95%. XRD patterns of BST samples (Supporting Information, Figure S5a) correspond to rhombohedral $Bi_{0.5}Sb_{1.5}Te_3$ patterns, and no peaks related to the oxidation and impurities were observed. On the other hand, XRD patterns of BST:T samples (Supporting Information, Figure S5b) show $Bi_{0.5}Sb_{1.5}Te_3$ patterns with tiny Te (101) peak, which can be attributed to excess Te. The peak intensity of Te (101) decreased with increasing NC glue contents and became negligible in BST:T3 and BST:T5 samples (Supporting Information, Figure S5b). This revealed the reaction between excessive Te and $Sb_2Te_7^{4-}$ MCC-capped Bi NCs during heat treatment and the formation of a $Bi_xSb_{2-x}Te_3$ phase at the interfaces.

We further studied hot-pressed BST samples by the energy dispersive X-ray spectroscopy (EDS). The TEM image and EDS spectra (Supporting Information, Figure S6) showed that the edge region of grinded particles have Bi-rich compared with the inside region, which clearly demonstrated the formation of interfaces from $Sb_2Te_7^{4-}$ MCC-capped Bi NCs between BiSbTe grains.

Figure 3 a,b show the hole concentrations (n_h) and mobilites (μ_h) obtained from Hall measurements at 300 K in samples with different amounts of NCs. Figure 3 a shows that the addition of NC glue increased n_h in BST samples from 2.1×10^{19} cm^{-3} to 8.3×10^{19} cm^{-3}. This indicates that $Sb_2Te_7^{4-}$ MCC-capped Bi NCs act as the p-type dopant for BST particles. As described above, the NC glue formed Bi-rich phase at interfaces in BiSbTe. Excessive Bi atoms are known to form Bi_{Te} antisite defects in BiSbTe, creating one additional free hole per defect.[16] In our case, it resulted in the formation of interfaces with additional p-doping compared to the grain interior. At the same time, μ_h slowly decreased as the amount of NC glue increased (Figure 3 a), which is presumably due to an increased scattering of holes on ionized antisite defects.

The BST:T samples showed the opposite and weaker dependence of n_h and μ_h on the NC content than those of BST samples, where the addition of NC glue caused a gradual decrease of n_h (Figure 3 b). Furthermore, the μ_h increased until 3 wt% of the NC glue content (Figure 3 b). As discussed above, the BST:T samples contained excess Te that suppressed the formation of Bi_{Te} antisite defects. Moreover, as observed in XRD patterns (Supporting Information, Figure S5b), this excessive Te reacted with excessive Bi from the NCs, forming near-stoichiometric $Bi_xSb_{2-x}Te_3$ at the interfaces with $x>0.5$. These interfaces can improve the electronic connectivity between grains, unlike the doped interfaces with ionized defects in BST samples, which can explain the increase of μ_h of the BST:T samples. Also, in stoichiometric $Bi_xSb_{2-x}Te_3$ phases, n_h generally decreases with an increase of x owing to suppression of the formation of Sb_{Te} antisite defects acting as p-type dopant. Accordingly, the Sb-poor but near stoichiometric interfaces formed by reacting Bi-rich NC glue with Te-rich BST:T particles are expected to behave as de-doped or un-doped interfaces with slightly lower n_h compared to the grain interior.

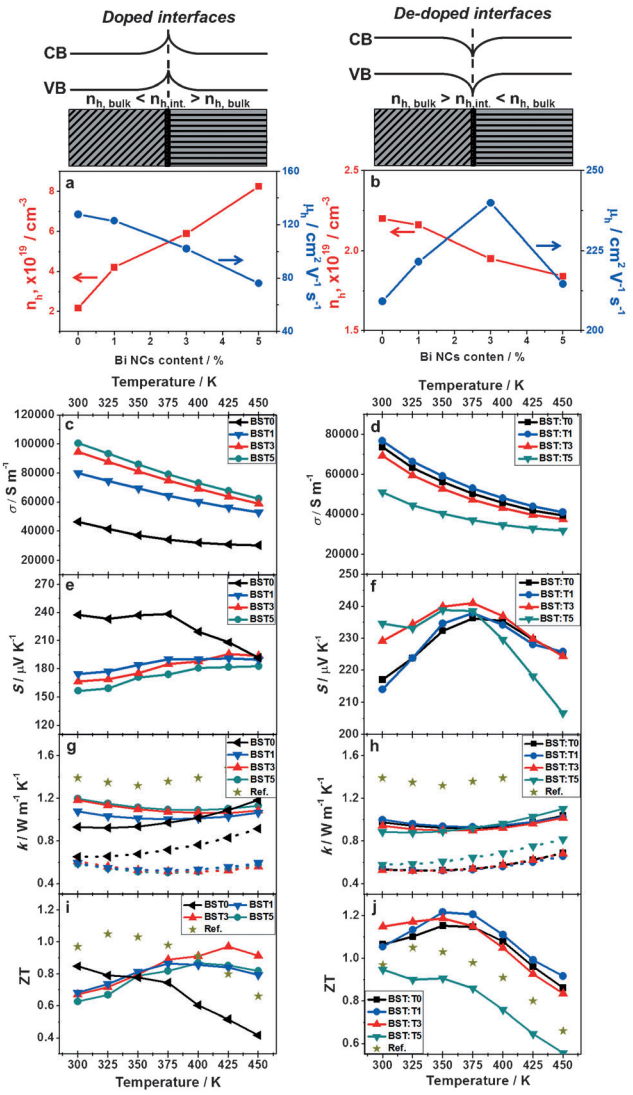

Figure 3. a,b) Plots of hole mobility and hole concentration versus Bi NC contents in a) BST and b) BST:T samples at 300 K. Temperature dependence for c,d) electrical conductivity, e,f) Seebeck coefficient, g,h) thermal conductivity (solid lines) and lattice contributions to thermal conductivity (dotted lines), and i,j) ZT values for BST samples (for (c), (e), (g), and (i)) and BST:T samples (for (d), (f), (h), and (j)), respectively. Stars in panels (g)–(j) indicate the corresponding data for the state-of-the-art BiSbTe bulk material.[3a] All lines are guides to the eye.

The TE properties of all BST and BST:T samples were measured at temperatures ranging from 300 K to 450 K. The additional doping of interfaces in BST samples significantly increased the overall electrical conductivity (σ), up to 110000 $S\,m^{-1}$ (Figure 3c) by introducing additional charge carriers. Near 300 K, the increase of n_h with the increase of NC content caused a decrease of the Seebeck coefficient (S), which reflected well-known behavior of heavily doped semiconductors.[4] At the same time, the addition of the NC glue changed the temperature dependence of S in BST samples: S of BST0 decreased with increasing T while all samples with doped interfaces showed $dS/dT > 0$ (Figure 3e). According to Lan et al,[17] Bi-rich phases in BiSbTe scatter minority carriers (electrons) more severely than holes and therefore suppress bipolar contribution of thermally generated electrons. Likewise, the Bi-rich doped interfaces in BST samples can suppress the bipolar effect and enhance S at elevated temperature.

The BST:T1 and BST:T3 samples with the interfaces de-doped or un-doped by the NC glue exhibited slightly higher or similar σ compared to the BST:T0 sample, reflecting an increase in μ_h by the NC glue effect (Figure 3d). Also, the S at room temperature generally increased with increasing the NC content (Figure 3f), which is consistent with decreased n_h arising from the de-doped interfaces. This increased σ or S resulted in the higher power factor of BST:T1 and BST:T3 compared to BST:T0. In BST:T5 sample, it showed a faster decrease of S than other samples at high temperature, which could originate from stronger bipolar contribution to S due to the low n_h.

The thermal conductivity (k) of BST and BST:T samples were significantly decreased in comparison to those of the state-of-the-art (SOA) bulk BiSbTe[3a] (Figure 3g and h) owing to nano- or mesostructuring.[18] Interestingly, k of the BST0 sample showed significant temperature dependence, whereas other BST samples showed almost constant k across the measured temperature range. Such a behavior of k can also be attributed to a suppressed bipolar effect at this temperature range by Bi-rich doped interfaces.[17] On the other hand, all BST:T samples showed similar behaviors to BST:T0 because of the formation of interfaces with stoichiometric $Bi_xSb_{2-x}Te_3$ phases.

The lattice thermal conductivity (k_L) of samples was calculated based on the equation of $k = k_E + k_L$, where k_E is electronic thermal conductivity estimated by the Wiedemann–Franz law of $k_E/\sigma = LT$. The Lorenz number (L) of $2.0 \times 10^{-8}\,V^2K^{-2}$ was used for heavily doped semiconductors.[19] In the BST samples, the k_L of all BST samples with doped interfaces (Figure 3g) was strongly decreased, indicating that Bi-rich interfaces effectively scatter phonons. On the other hand, the BST:T samples exhibited similar k_L regardless of NC content except for the BST:T5 sample (Figure 3h), revealing the formation of smooth interfaces with a similar phase to bulk matrix from the NC glue. The high k_L of BST:T5 may indicate that the smoother and thicker interfaces provided a new phonon transport channel rather than phonon scattering sites.

The dimensionless figure-of-merit ZT values for all of the samples were estimated from the measured σ, S, and k values. The thermal conductivities of the samples were measured along the direction parallel to the pressing, whereas the electrical properties were measured along the perpendicular direction. Generally, Bi_2Te_3 based materials can exhibit anisotropic thermoelectric properties owing to anisotropic crystal structures. However, the anisotropy of nanostructured materials can be considerably decreased because of the random orientation of nanoparticle building blocks.[3a] Our BST and BST:T samples also showed the isotropic crystal structures and electrical properties (the detailed explanation and data are described in the Supporting Information), which confirm that the calculated ZT values were not overestimated.

The decreased thermal conductivities and enhanced power factors led to significantly enhanced ZT values of BST samples with doped interfaces in comparison to BST0 (Figure 3i). The highest ZT of about 1 was achieved by BST3 at 425 K. All of the BST samples with doped interfaces showed peak ZT values above 400 K, in contrast to a peak ZT at 325 K for BST0, which is most likely due to the decreased bipolar effect.[3a,17] Above 400 K, all BST samples containing the NC glue showed higher ZT values compared to SOA bulk BiSbTe. On the other hand, BST:T1 samples exhibited similar temperature dependence of ZT to BST:T0, and the peak ZT values of other samples moved to lower temperature with increasing NC content (Figure 3j), which is attributable to the decrease of n_h by the formation of de-doped interfaces. Furthermore, the enhanced power factors of BST:T1 and BST:T3 by increased μ_h arising from the smooth interfaces led to circa 10% higher ZT values compared to BST:T0. BST:T1 exhibited the highest ZT of 1.22 at 350 K and $ZT > 1$ over a wide temperature range from 300 K to 425 K.

As a consequence, the formation of Bi-rich doped interfaces from the NC glue in pure $Bi_{0.5}Sb_{1.5}Te_3$ grains led to the remarkable change of electrical and thermal properties, resulting in the large increase of ZT at elevated temperatures. On the other hand, the de-doped interfaces with stoichiometric $Bi_xSb_{1-x}Te_3$ phases improved the electronic connectivity between BiSbTe grains and increased μ_h, eventually enhancing the power factors and ZT. So, the current approach to use all-inorganic NCs as glue for BiSbTe grains shows the diverse way to control TE properties by designing and engineering the interfaces.

In summary, we have shown the enhanced TE performance of materials prepared from ball-milled BiSbTe particles mixed with inorganic NC glue. $Sb_2Te_7^{4-}$ MCC capped Bi NCs filled up voids and interfaces between particles and joined them together by preferential sintering. The NC glue helped connect grains of TE material without applying high temperature and pressure, enabling solution processed BiSbTe thin films and pellets. The effect of the NC glue can be particularly useful for making thin-film TE modules for site-selective cooling of microdevices.[4,20] Furthermore, we showed that the NC glue can be used for selectively tailoring the doping in vicinity of the interfaces in mesostructured TE materials. Similar NC-based chemistry can be used to introduce different elements and rationally engineer both electron and phonon transport. We strongly believe that the

engineering of the grain boundaries in TE materials will become a powerful and commonly used approach.

Received: February 3, 2014
Published online: May 22, 2014

Keywords: bismuth · interfaces · nanostructures · semiconductors · thermoelectric materials

[1] a) A. J. Minnich, M. S. Dresselhaus, Z. F. Ren, G. Chen, *Energy Environ. Sci.* **2009**, *2*, 466 – 479; b) J. R. Sootsman, D. Y. Chung, M. G. Kanatzidis, *Angew. Chem.* **2009**, *121*, 8768 – 8792; *Angew. Chem. Int. Ed.* **2009**, *48*, 8616 – 8639.
[2] a) K. F. Hsu, S. Loo, F. Guo, W. Chen, J. S. Dyck, C. Uher, T. Hogan, E. K. Polychroniadis, M. G. Kanatzidis, *Science* **2004**, *303*, 818 – 821; b) K. Biswas, J. He, I. D. Blum, C.-I. Wu, T. P. Hogan, D. N. Seidman, V. P. Dravid, M. G. Kanatzidis, *Nature* **2012**, *489*, 414 – 418.
[3] a) B. Poudel, Q. Hao, Y. Ma, Y. C. Lan, A. Minnich, B. Yu, X. A. Yan, D. Z. Wang, A. Muto, D. Vashaee, X. Y. Chen, J. M. Liu, M. S. Dresselhaus, G. Chen, Z. F. Ren, *Science* **2008**, *320*, 634 – 638; b) X. A. Yan, B. Poudel, Y. Ma, W. S. Liu, G. Joshi, H. Wang, Y. C. Lan, D. Z. Wang, G. Chen, Z. F. Ren, *Nano Lett.* **2010**, *10*, 3373 – 3378.
[4] G. J. Snyder, E. S. Toberer, *Nat. Mater.* **2008**, *7*, 105 – 114.
[5] W. Kim, R. Wang, A. Majumdar, *Nano Today* **2007**, *2*, 40 – 47.
[6] J. H. Yang, H. L. Yip, A. K. Y. Jen, *Adv. Energy Mater.* **2013**, *3*, 549 – 565.
[7] a) Y. Yan, R. Noufi, M. M. Al-Jassim, *Phys. Rev. Lett.* **2006**, *96*, 205501; b) J. R. Sites, J. E. Granata, J. F. Hiltner, *Sol. Energy Mater. Sol. Cells* **1998**, *55*, 43 – 50.
[8] L. Xiangxin, A. D. Compaan, J. Terry in Photovoltaic Specialists Conference, **2005**. Conference Record of the Thirty-first IEEE, **2005**, pp. 267 – 270.
[9] U. Rau, K. Taretto, S. Siebentritt, *Appl. Phys. A* **2009**, *96*, 221 – 234.
[10] Y. Ma, Q. Hao, B. Poudel, Y. C. Lan, B. Yu, D. Z. Wang, G. Chen, Z. F. Ren, *Nano Lett.* **2008**, *8*, 2580 – 2584.
[11] J. S. Son, K. Park, M. K. Han, C. Kang, S. G. Park, J. H. Kim, W. Kim, S. J. Kim, T. Hyeon, *Angew. Chem.* **2011**, *123*, 1399 – 1402; *Angew. Chem. Int. Ed.* **2011**, *50*, 1363 – 1366.
[12] M. V. Kovalenko, B. Spokoyny, J. S. Lee, M. Scheele, A. Weber, S. Perera, D. Landry, D. V. Talapin, *J. Am. Chem. Soc.* **2010**, *132*, 6686 – 6695.
[13] J. W. G. Bos, H. W. Zandbergen, M. H. Lee, P. Ong, R. J. Cava, *Phys. Rev. B* **2007**, *75*, 195203.
[14] E. A. Olson, M. Y. Efremov, M. Zhang, Z. Zhang, L. H. Allen, *J. Appl. Phys.* **2005**, *97*, 034304.
[15] K. Hasezaki, M. Nishimura, M. Umata, H. Tsukuda, M. Araoka, *Mater. Trans.* **1994**, *35*, 428 – 432.
[16] W. S. Liu, Q. Y. Zhang, Y. C. Lan, S. Chen, X. Yan, Q. Zhang, H. Wang, D. Z. Wang, G. Chen, Z. F. Ren, *Adv. Energy Mater.* **2011**, *1*, 577 – 587.
[17] Y. C. Lan, B. Poudel, Y. Ma, D. Z. Wang, M. S. Dresselhaus, G. Chen, Z. F. Ren, *Nano Lett.* **2009**, *9*, 1419 – 1422.
[18] J. P. Feser, E. M. Chan, A. Majumdar, R. A. Segalman, J. J. Urban, *Nano Lett.* **2013**, *13*, 2122 – 2127.
[19] H. J. Goldsmid, *Electronic refrigeration*, Pion, London, **1986**.
[20] I. Chowdhury, R. Prasher, K. Lofgreen, G. Chrysler, S. Narasimhan, R. Mahajan, D. Koester, R. Alley, R. Venkatasubramanian, *Nat. Nanotechnol.* **2009**, *4*, 235 – 238.

